AMMCA: Acoustic Massive MIMO with Carrier Aggregation to Boost the Underwater Communication Data Rate

Xueyuan Zhao and Dario Pompili
Department of Electrical and Computer Engineering
Rutgers University–New Brunswick, NJ, USA
E-mails: xueyuan_zhao@cac.rutgers.edu, pompili@ece.rutgers.edu

ABSTRACT

A new communication approach based on massive Multiple Input Multiple Output (MIMO) with Carrier Aggregation (CA), named AMMCA, is proposed to boost the achievable data rate for multimedia traffic in underwater acoustic channels. The system under study is composed of a surface buoy station with many hydrophones and of an underwater static or mobile node such as an Autonomous Underwater Vehicle (AUV) with a few transducers. The proposed idea presents two components: (i) the first consists in deploying a large number of hydrophones at the buoy for uplink massive MIMO reception; (ii) the second requires employing carrier aggregation of Orthogonal Frequency Division Multiplexing (OFDM) symbols to exploit a wider underwater bandwidth than in traditional acoustic systems that use only a few tens of KHz. Via both theoretical analysis and computer-based simulations, AMMCA is shown to boost the achievable data rate in underwater acoustic channels for both medium/short and long distances.

Keywords

Underwater Acoustic Communications; Massive MIMO; Carrier Aggregation; OFDM; Achievable Data Rate.

1. INTRODUCTION

Motivations: Existing underwater acoustic communication systems can only support low-rate, low-quality video transmissions, e.g., in the order of 64 Kbit/s rates [1], whereas high-quality video transmissions require a higher bit rate, i.e., in the Mbit/s scale for MPEG-1 compressed video. And yet, the acoustic data rate achievable with state-of-the-art communication systems is still far from sufficient to support such high-quality video streaming applications. In [1], the achievable rate of an acoustic underwater system is reported to be 150 Kbit/s over a short vertical path at a carrier frequency of 75 KHz. Another acoustic system [2] achieves a rate of 125.7 Kbit/s over the bandwidth of 62.5 KHz.

To address this critical data-rate issue, recent proposals focus on laser- and Light Emitting Diode (LED)-based underwater communication systems that can achieve Mbit/s data rates. In [3], the proposed laser-based system can achieve a few Mbit/s on short distances and has a maximum distance of 300 to 400 meters. In [4], the LED-based underwater system can achieve few Mbit/s over a few meters. While these systems achieve high data rates, their coverage ranges are much smaller than those needed in real underwater communication systems. Moreover, for laser-based systems, the positioning of the laser transmitters/receivers as well as the shadowing of the laser beam caused by ocean lives can significantly affect the overall communication rate. In contrast, acoustic waves can propagate tens of kilometers and are suitable for long-distance underwater communications. In this paper, we propose a new achievable rate-improvement method based on massive Multiple Input Multiple Output (MIMO) reception and Orthogonal Frequency Division Multiplexing (OFDM) carrier aggregation. We target to improve the achievable rate by an order of magnitude compared with existing acoustic systems in such a way as to meet the requirements of high-quality, real-time video transmission.

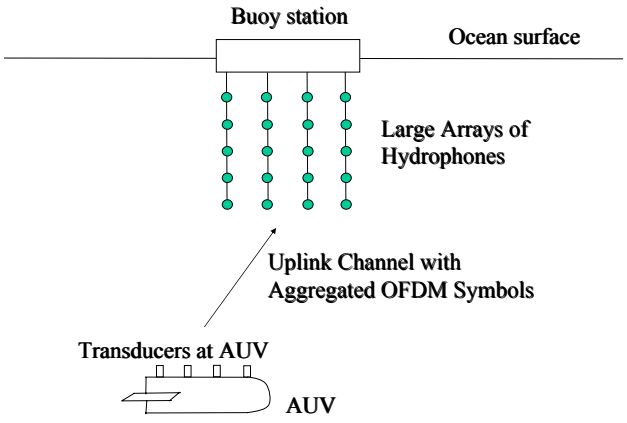

Figure 1: Underwater acoustic communication system under study, where a large number of hydrophones are deployed at the buoy station to support massive MIMO at the receiver.

Related Work: Existing works on achievable rate improvement in underwater acoustic systems are based on MIMO and OFDM. In [5], a MIMO-OFDM system for underwater communications is proposed and the error rate performance is simulated. The system is evaluated for 4-by-4 MIMO settings by simulation with Zero-Forcing (ZF) symbol detection. Other existing underwater MIMO proposals are all limited to a small number of acoustic transceivers such as in [6]. The existing underwater testbeds also assume a

WUWNET'15, October 22-24 2015, Washington DC, USA

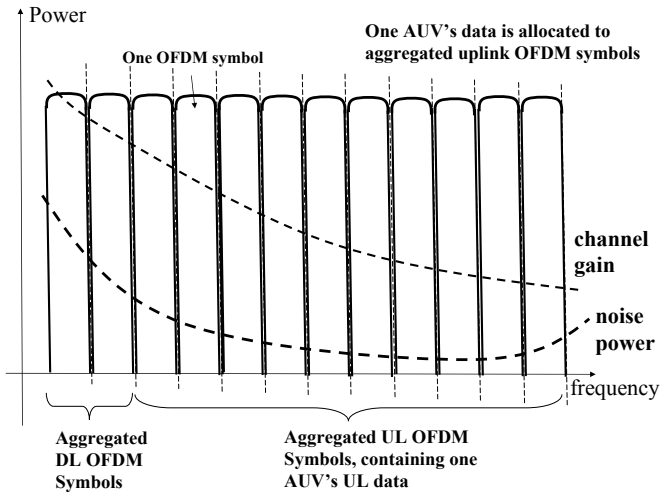

Figure 2: Proposed OFDM Carrier Aggregation (CA) for Up-Link (UL) and DownLink (DL) transmissions.

small number of transceivers [7]. Existing works on underwater MIMO systems are limited to conventional MIMO, where the number of acoustic units at both transmitter and receiver is small. Also, existing works assume single OFDM carrier. Although carrier aggregation and massive MIMO have been studied for terrestrial communication systems [8, 9], there is no work on underwater acoustic OFDM carrier aggregation and massive MIMO hydrophone receivers for underwater acoustics. In our paper, we propose a new approach that is able to support carrier aggregation and massive MIMO reception, where the objective is to enable $\mathrm{Mbit/s}$ real-time, high-quality underwater UpLink (UL) video transmission from a static or mobile node such as an Autonomous Underwater Vehicle (AUV) to a surface buoy station (Fig. 1).

Our Contributions: Our proposal consists in utilizing a wide bandwidth by transmitting multiple OFDM symbols, as depicted in Fig. 2. The available bandwidth is partitioned into N_{OFDM} carriers, where each carrier has one OFDM symbol. There are N_{UL} OFDM symbols allocated for the UL transmission and N_{DL} symbols for the DownLink (DL) transmission, where clearly $N_{OFDM} = N_{UL} + N_{DL}$. The N_{UL} symbols are aggregated and assigned to one AUV's transmission. Assume there are N_{subc} subcarriers in one OFDM symbol, composed of $N_{subc} = N_{data}+N_{pilot}+N_{null}$, where N_{data} is the number of data subcarriers, N_{pilot} the number of pilot subcarriers, and N_{null} the number of null subcarriers. The total number of data subcarriers for the UL transmission is $N_{ch} = N_{data}N_{UL}$ for the carrier-aggregated system. The allocation of uplink and downlink OFDM symbols in frequency depends on the type of data traffic. For underwater AUV applications, it is expected that the uplink has real-time video or data-packet transmission requirements, whereas the downlink may contain commands that require less bandwidth than for the uplink case.

Another key aspect of our proposal is the massive MIMO reception. If the number of hydrophones at the buoy is N_R and the number of transducers at an AUV is N_T, the proposed massive MIMO reception assumes $N_R \gg N_T$. In practice, N_R is expected to be one order of magnitude larger than N_T. The proposed massive MIMO buoy receiver is depicted in Fig. 1. The massive MIMO hydrophone array is realized by multiple ironic poles, each with an array of hydrophones. The feasibility of the proposal for massive MIMO is based on available acoustic array technology that supports very large number of acoustic hydrophones. An acoustic sensor array of 96 hydrophones has been built using fiber-optic interferometric acoustic sensors [10]. This sensor technology can replace the electro-ceramic transducers sonar array for the massive MIMO system in underwater cellular networks. Existing commercial hydrophones are also of low cost and high bandwidth, ranging in 10-500 KHz. These hydrophones can be deployed with hard ironic poles. Multiple poles are deployed with hydrophones attached on. This can construct an implementation of the large number of hydrophones at the surface buoy.

In this proposal, we aim at obtaining a significant and quantifiable improvement in terms of achievable data rate. The key contributions and findings of our work are:

- Closed-form theoretical result is derived for the system given Zero-Forcing (ZF) detection at the buoy receiver;
- Achievable rate is improved for medium/short distances by carrier aggregation based on a higher utilization of the scarce underwater spectrum compared with acoustic MIMO-OFDM systems with no carrier aggregation;
- Achievable rate is improved for long distances by adopting acoustic massive MIMO to increase the post-detection Signal-to-Noise Ratio (SNR) compared with acoustic MIMO-OFDM systems with no massive MIMO deployment.

Overall, the proposed AMMCA can significantly improve the achievable rate for *both* medium/short and long distances.

Paper Organization: In Sect. 2, the theoretical rate of the system is mathematically derived; computer simulation results are then given in Sect. 3; finally, conclusions are drawn in Sect. 4.

2. THEORETICAL ACHIEVABLE RATE

We derive here the theoretical achievable rate of the proposed approach. The system under study has one surface buoy station with N_R hydrophone receivers, and one AUV with N_T transducers. Assume the total number of subchannels is $N_{ch} = N_{data}N_{UL}$. For the k-th subchannel, where $k = 1, 2, ..., N_{ch}$, the received signal power at the buoy, in dBm, can be expressed as $P_S(k) = P_{Tx}(k) - A(k) + G(k)$, where $P_{Tx}(k)$ is the AUV transmitting power, which includes power allocation for the k-th subchannel, $A(k)$ is the large-scale channel attenuation, and $G(k)$ is the directional gain.

The noise power at the buoy, in dBm, can be written as $P_N(k) = P_{AN}(k)+P_{CN}(k)$, where $P_{AN}(k)$ is the ambient noise power and $P_{CN}(k)$ is the circuit noise power, which includes the hydrophone front-end noises. For a Single Input Single Output (SISO) channel, the SNR of the k-th subchannel, in linear scale, is computed as $\rho(k) = 10^{[P_S(k)-P_N(k)]/10}$. This SNR includes the effects of power allocation, large-scale path loss, transducer gain, and ambient as well as circuit noise. The information-theoretical rate at the k-th subchannel of a SISO system, normalized to a unit of bandwidth, is $C_{SISO}(k) = \log_2[1 + \rho(k)]$, where the unit is $\mathrm{bps/Hz}$.

To calculate the rate of all the N_{ch} subchannels, we sum the rate of all subchannels by multiplying the subchannel width, i.e.,

$$R_{UL,SISO}(k) = \beta\lambda\eta \cdot \sum_{k=1}^{N_{ch}} [C_{SISO}(k) \cdot \Delta f]. \quad (1)$$

The parameter β is the ratio of UL frequency OFDM symbols to all the available UL and DL frequency OFDM symbols; the parameter λ is the ratio of data subcarriers to all the subcarriers in one OFDM symbol; the parameter η represents the cyclic prefix causing efficiency reduction; finally, Δf is the subcarrier spacing. The unit

of $R(k)$ is bps and represents the theoretical limit for uplink data transmission of a SISO system.

Now, for a massive MIMO system, assuming the receiver uses ZF detection and the MIMO channel response of the k-th subchannel is $\mathbf{H}(k)$, the ZF detection matrix for the k-th subchannel is,

$$\mathbf{G}(k) = (\mathbf{H}^H(k)\mathbf{H}(k))^{-1}\mathbf{H}^H(k), \tag{2}$$

and the received signal $\mathbf{y}(k)$ at the buoy station after ZF detection can be written as,

$$\begin{aligned}\mathbf{y}(k) &= \mathbf{G}(k)(\mathbf{H}(k)\mathbf{x}(\mathbf{k}) + \mathbf{n}) \\ &= \mathbf{x}(k) + (\mathbf{H}^H(k)\mathbf{H}(k))^{-1}\mathbf{H}^H(k)\mathbf{n},\end{aligned} \tag{3}$$

where $\mathbf{x}(k)$ is the signal vector transmitted on the k-th subchannel and $\mathbf{n}$ is the Additive White Gaussian Noise (AWGN) vector. Defining matrix $\mathbf{W}(k) = \mathbf{H}^H(k)\mathbf{H}(k)$, the covariance matrix of the filtered noise vector is,

$$\begin{aligned}&\mathbf{R_n} = (\mathbf{H}^H(k)\mathbf{H}(k))^{-1}\mathbf{H}(k)^H\cdot \\ &E\{\mathbf{n}\mathbf{n}^H\}\mathbf{H}(k)\left[(\mathbf{H}^H(k)\mathbf{H}(k))^{-1}\right]^H \\ &= (\mathbf{H}^H(k)\mathbf{H}(k))^{-1} = \mathbf{W}^{-1}(k).\end{aligned} \tag{4}$$

From (3), the post-detection SNR on the i-th stream of the k-th subchannel is,

$$\gamma_i(k) = \frac{\rho(k)}{N_T\left[\mathbf{W}^{-1}(k)\right]_{i,i}}, \tag{5}$$

where the spatial stream index $i = 1, ..., N_{SS}$, and N_{SS} is the number of spatial streams sent by the AUV transmitter. The ergodic capacity for the k-th subchannel can be written as,

$$C_{ZF}(k) = E\left\{\sum_{i=1}^{N_{SS}} \log_2\left[1 + \gamma_i(k)\right]\right\}, \tag{6}$$

and the achievable rate for the OFDM-based uplink channels can be expressed by,

$$R_{UL,ZF}(k) = \beta\lambda\eta \cdot \sum_{k=1}^{N_{ch}} [C_{ZF}(k) \cdot \Delta f], \tag{7}$$

where β, λ, and η are defined as in the SISO case.

The ergodic capacity $C_{ZF}(k)$ can be further expressed as,

$$\begin{aligned}C_{ZF}(k) &= E\left\{\sum_{i=1}^{N_{SS}} \log_2\left[1 + \gamma_i(k)\right]\right\} \\ &= \sum_{i=1}^{N_{SS}} E\left\{\log_2\left[1 + \gamma_i(k)\right]\right\} \\ &= \sum_{i=1}^{N_{SS}} \int \log_2\left[1 + \gamma_i(k)\right] p_{\gamma_i(k)} d\gamma_i(k),\end{aligned} \tag{8}$$

where $p_{\gamma_i(k)}$ is the Probability Density Function (PDF) of $\gamma_i(k)$. Note that the PDF of ZF post-detection $\gamma_i(k)$ is gamma distributed [11] and has the parameters of $Gamma(N, \varphi(k))$, where $N = N_R - N_T + 1$ and $\varphi(k) = \rho(k)/N_T$. The PDF of variable $\gamma_i(k)$ is,

$$p_{\gamma_i(k)} = \frac{(\gamma_i(k))^{N-1} e^{-\gamma_i(k)/\varphi(k)}}{(N-1)!\varphi(k)^N}. \tag{9}$$

By replacing the PDF with the above gamma distribution, the expression of $C_{ZF}(k)$ can be rewritten as,

$$\begin{aligned}&C_{ZF}(k) = \tfrac{(N-1)!\varphi(k)^N}{\log(2)}\cdot \\ &\sum_{i=1}^{N_{SS}} \int_0^{+\infty} \ln\left[1 + \gamma_i(k)\right](\gamma_i(k))^{N-1} e^{-\gamma_i(k)/\varphi(k)} d\gamma_i(k).\end{aligned} \tag{10}$$

By Taylor series expansion, $\ln\left[1 + \gamma_i(k)\right]$ can be written as,

$$\ln\left[1 + \gamma_i(k)\right] = \sum_{n=1}^{+\infty} (-1)^{n-1} \frac{(\gamma_i(k))^n}{n}. \tag{11}$$

For tractability, we adopt the infinite expansion of log function and rewrite the term $C_{ZF}(k)$ as,

$$\begin{aligned}&C_{ZF}(k) = \tfrac{(N-1)!\varphi(k)^N N_{SS}}{\ln(2)}\cdot \\ &\sum_{m=1}^{+\infty}\left\{(-1)^{m+1}\tfrac{1}{m}(\varphi(k))^{N+m}\,\Gamma(N+m)\right\}.\end{aligned} \tag{12}$$

Finally, the uplink achievable rate can be expressed exactly in closed-form as in the following theorem.

Theorem 1: Achievable rate of the AMMCA system. The achievable rate can be expressed as,

$$\begin{aligned}&R_{UL,ZF} = \beta\lambda\eta\tfrac{(N-1)!N_{SS}}{\ln(2)}\cdot \\ &\sum_{k=1}^{N}\left[\varphi(k)^N \sum_{m=1}^{+\infty}\left\{(-1)^{m+1}\tfrac{1}{m}(\varphi(k))^{N+m}\,\Gamma(N+m)\right\}\cdot\Delta f\right],\end{aligned} \tag{13}$$

where N is defined as $N = N_R - N_T + 1$; N_{SS} is the number of spatial streams; $\varphi(k)$ is the gamma distribution parameter $Gamma(N, \varphi(k))$ of random variable (r.v.) $\gamma_i(k)$; β is the ratio of UL frequency bands; λ is the ratio of data subcarriers; η is the cyclic prefix causing efficiency reduction; Δf is the subcarrier spacing; and $\Gamma()$ is the Euler gamma function.

3. PERFORMANCE EVALUATION

We discuss now the performance evaluation of our proposed approach. We first describe the simulation conditions, including the acoustic channel and noise models used in our simulations; then, we present the computer-based simulation results and provide insights on the performance gain.

Acoustic Channel Model and Noise Model: Bellhop Simulator and Acoustic Channel Simulator are available for acoustic signal-propagation simulations. The Bellhop model [12] is based on acoustic ray tracing and can generate transmission loss, eigen rays, arrivals, and received time-series for a wide frequency range. The inputs include sound-speed profile, bottom-reflection coefficient, top-reflection coefficient, source-beam pattern. The Acoustic Channel Simulator in [13] can generate both large-scale and small-scale variations, where the former can be estimated using the Bellhop Simulator.

Our simulations use the following parameters. The water depth is 5000 m; the transmitting AUV, which is assumed to be static, has a depth of 1000 m and the receiving hydrophone has a depth of 5 m. The distance between the AUV and buoy is varied from 1 to 25 km, with a space granularity of 1 km. The attenuation for large-scale fading is firstly generated by the Bellhop Simulator; then, the effect of sound frequency-dependent attenuation is added.

The underwater acoustic noise is composed of four major noise sources – turbulence, shipping, waves, and thermal noise [14, 15]. The noise spectrum densities of the four types of noise are frequency dependent. The ambient noise is the summation of these four noise sources, and is frequency dependent (i.e., it is "colored"). We have adopted this acoustic-noise model in our simulations.

Transducer and Hydrophone Simulation Assumptions: We assume the transmitter uses a transmitting power of 160 dB re μPa and produces acoustic waves from 10 to 500 KHz. The transmitting power is in the scale of hundred of dB re μPa [14]. To meet the independent-received-signal assumption, the spacing of the hydrophones should be greater than the wavelength. A realistic

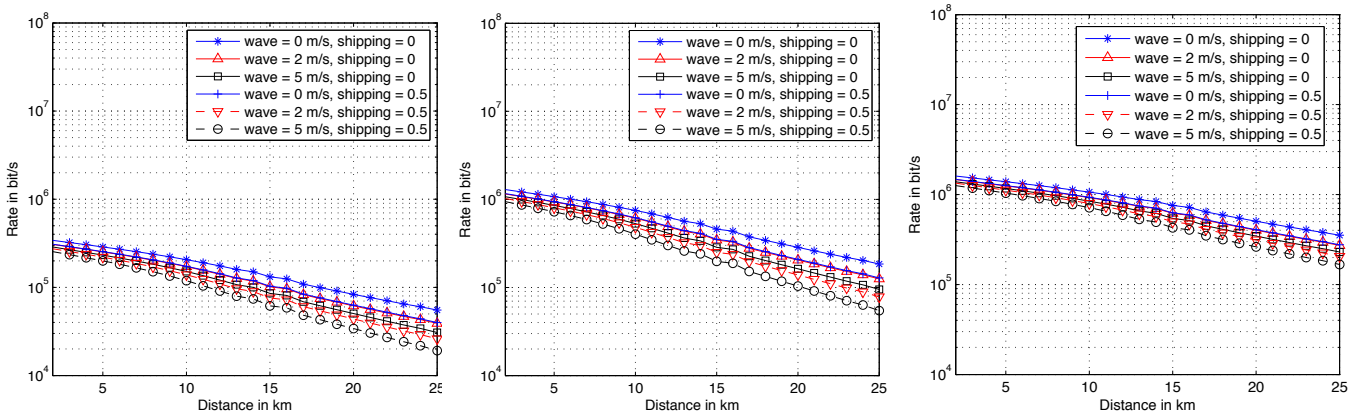

(a) (b) (c)

Figure 3: UpLink (UP) achievable rate for (a) 1-by-1 SISO without carrier aggregation, (b) 4-by-4 MIMO without carrier aggregation, and (c) massive MIMO without carrier aggregation. For (c), there are 4 transducers at the AUV and 100 hydrophones at the surface buoy. The distances of all results range from 2 to 25 km.

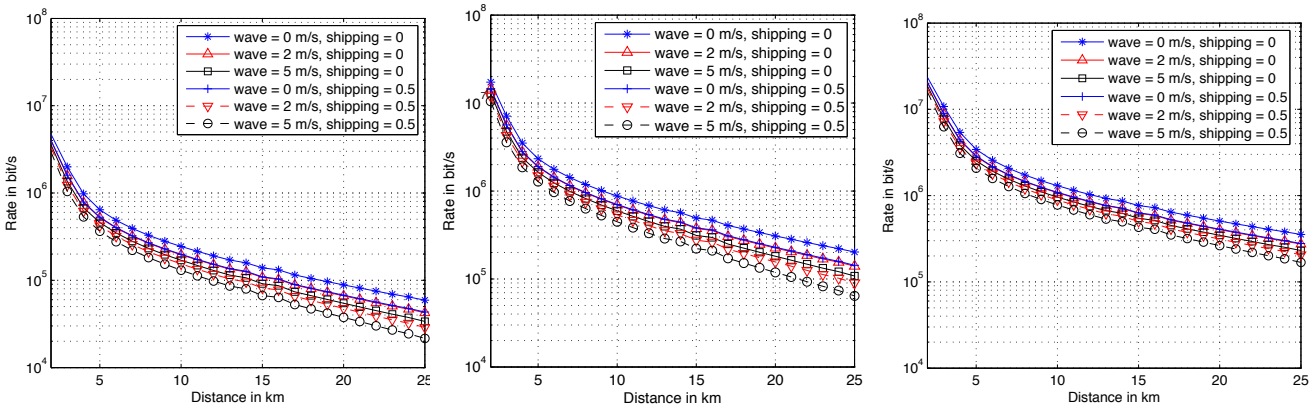

(a) (b) (c)

Figure 4: UpLink (UP) achievable rate for (a) 1-by-1 SISO with carrier aggregation (SISO-CA), (b) 4-by-4 MIMO with carrier aggregation (MIMO-CA), and (c) massive MIMO with carrier aggregation (AMMCA). For AMMCA in (c), there are 4 transducers at the AUV and 100 hydrophones at the surface buoy. The distances of all results range from 2 to 25 km.

and conservative estimate for the wavelength is 0.15 m for a carrier frequency of 10 KHz and sound speed of 1500 m/s. With a higher carrier frequency, the wavelength – and therefore the minimum spacing between hydrophones – decrease. The hydrophone can be constructed with inter-element spacing greater than 0.15 m for receiving acoustic signals that can be considered independent.

OFDM Simulation Assumptions: The OFDM system parameters are chosen according to a common underwater multipath delay profile. The multipath has a maximum delay of τ_{max}. The length of cyclic prefix T_{CP} is related with the length of the OFDM symbol T_{OFDM} as $T_{OFDM} = \alpha T_{CP}$, where α is a constant. We choose the cyclic prefix length to be 20 ms, the OFDM symbol length to be 100 ms, and the subcarrier spacing to be 10 Hz. We assume the OFDM Fast Fourier Transform (FFT) size of 2048, and the OFDM system bandwidth to be 20.48 KHz. The number of OFDM data subcarriers is assumed to be 1500, given a 2048 total subcarriers including data, pilots, and null subcarriers. In the simulations, FFT size and CP length are fixed; this is because practical systems generally adopt fixed FFT size and CP length.

For Carrier Aggregation (CA), let us assume that a frequency ranging from 10 to 500 KHz is allocated for the uplink transmission. There are 24 OFDM symbols aggregated for both the uplink and downlink transmissions. From 0 to 10 KHz, the noise level is high; plus, marine lives communicate using this band. Avoiding this band can therefore reduce interference to the communication of marine lives. The ratio of data subcarriers is $\lambda = 1500/2048$. The cyclic prefix causing efficiency reduction is $\eta = 80$ ms$/100$ ms $= 0.8$. For carrier aggregation, the ratio of UL frequency OFDM bands β is assumed to be 80%.

We have chosen the zero-forcing detection algorithm. This is because in order to implement detection based on Minimum Mean Square Error (MMSE), noise variance estimation would be required; also, MMSE is sensitive to the noise variance estimation error. The post-detection SNR $\gamma_i(k)$ is computed for every subcarrier and every OFDM symbol. We define L_1 as the coding loss and L_2 as the loss of adaptive modulation. The SNR $\gamma_i(k)$ is deduced by the losses as $L = L_1 + L_2$ before achievable rate evaluation. We have assumed 6 dB for both the coding loss and for the loss of adaptive

modulation.

Simulation Results: Results obtained via computer simulations are depicted in Figs. 3 and 4. It can be observed that carrier aggregation significantly improves the achievable rate for medium/short distances less than 5 km for SISO, MIMO, and massive MIMO. For longer distances, i.e., from 10 to 25 km, carrier aggregation only slightly improves the achievable rate performance. The reason that only in medium/short distances CA performance is significantly improved is that, at such distances, the SNRs of OFDM symbols located at high frequencies are high (due to a low transmission loss), thus leading to a good achievable rate. Conversely, at long distances, the SNRs of OFDM symbols located at high frequencies are low, thus leading to marginal achievable rates. Therefore, for long distances, carrier aggregation cannot significantly improve the achievable rate performance.

As for massive MIMO, it can be observed from Figs. 3(b) and 3(c) that, compared with the traditional MIMO scheme, massive MIMO can improve the performance for long distances beyond 5 km; however, it cannot significantly improve performance for short/medium distances, i.e., within 5 km. The reason that massive MIMO cannot significant improve the achievable rate for medium and short distance is that the SNRs for a MIMO system at these distances are already very good (> 20 dB). Massive MIMO can significantly improve the post-detection SNR, but in the high-SNR region this SNR improvement does not translate into a significant rate improvement. In contrast, in the medium to low SNR region, the improvement of post-detection SNR by massive MIMO does result in significant rate improvement. Therefore, the benefit of massive MIMO is significant at long distances where the post-detection SNR is low. Note that, in all the simulation results, a non-flat bathymetry causes the unevenness of the curves with respect to the distances, as shown in all the results.

As for our proposed scheme, AMMCA, we note that it can improve the system for *both* within 5 km and beyond. It can be observed that, for 2 km distances, AMMCA and MIMO-CA have higher achievable rates than MIMO and SISO. At longer distances than 10 km, AMMCA and massive MIMO have higher rates than MIMO and SISO. We can conclude that our proposed AMMCA scheme retains both the benefits of MIMO-CA at short distance and those of massive MIMO at long distance, thus achieving the best performance among all schemes.

4. CONCLUSION

We proposed a new communication approach, AMMCA, suitable for multimedia traffic, which is based on massive MIMO with Carrier Aggregation (CA) of Orthogonal Frequency Division Multiplexing (OFDM) symbols. AMMCA's goal is to boost the achievable data rate for multimedia traffic in underwater acoustic channels. The major findings of this work include: (i) a closed-form theoretical result of the achievable data rate for the proposed scheme is derived given Zero-Forcing (ZF) detection at the surface buoy receiver; (ii) carrier aggregation is found to improve the achievable rate for medium/short distances; and (iii) massive MIMO is shown to improve the achievable rate for long distances. To sum up, via both theoretical analysis and computer-based simulations, we showed that AMMCA can boost significantly the achievable data rate in underwater acoustic channels for both medium/short and long distances.

Acknowledgment: This work was supported by the NSF CAREER Award No. OCI-1054234.

5. REFERENCES

[1] C. Pelekanakis, M. Stojanovic, and L. Freitag, "High rate acoustic link for underwater video transmission," in *IEEE OCEANS*, vol. 2, Sept 2003, pp. 1091–1097.

[2] B. Li, J. Huang, S. Zhou, K. Ball, M. Stojanovic, L. Freitag, and P. Willett, "MIMO-OFDM for high-rate underwater acoustic communications," *IEEE Journal of Oceanic Engineering*, vol. 34, no. 4, pp. 634–644, Oct 2009.

[3] Y. Chen, X. Hu, D. Wang, H. Chen, C. Zhan, and H. Ren, "Researches on underwater transmission characteristics of blue-green laser," in *IEEE OCEANS*, April 2014, pp. 1–5.

[4] A. Tennenbaum, M. Dyakiw, J.-H. Cui, and Z. Peng, "Application of low cost optical communication systems to underwater acoustic networks," in *IEEE International Conference on Mobile Ad Hoc and Sensor Systems (MASS)*, Oct 2014, pp. 755–758.

[5] I. Nelson, K. Vishvaksenan, and V. Rajendran, "Performance of turbo coded MIMO-OFDM system for underwater communications," in *International Conference on Communications and Signal Processing (ICCSP)*, April 2014, pp. 1735–1739.

[6] P.-J. Bouvet, Y. Auffret, A. Loussert, P. Tessot, G. Janvresse, and R. Bourdon, "MIMO underwater acoustic channel characterization based on a remotely operated experimental platform," in *IEEE OCEANS*, April 2014, pp. 1–6.

[7] R. Martins, J. Borges de Sousa, R. Caldas, C. Petrioli, and J. Potter, "SUNRISE project: Porto university testbed," in *Underwater Communications and Networking (UComms)*, Sept 2014, pp. 1–5.

[8] Y. Rui, P. Cheng, M. Li, Q. Zhang, and M. Guizani, "Carrier aggregation for LTE-advanced: uplink multiple access and transmission enhancement features," *IEEE Wireless Communications*, vol. 20, no. 4, pp. 101–108, August 2013.

[9] J. Hoydis, S. ten Brink, and M. Debbah, "Massive MIMO in the UL/DL of cellular networks: How many antennas do we need?" *IEEE Journal on Selected Areas in Communications*, vol. 31, no. 2, pp. 160–171, February 2013.

[10] G. Cranch, P. Nash, and C. Kirkendall, "Large-scale remotely interrogated arrays of fiber-optic interferometric sensors for underwater acoustic applications," *IEEE Sensors Journal*, vol. 3, no. 1, pp. 19–30, Feb 2003.

[11] D. Gore, R. Heath, and A. Paulraj, "Transmit selection in spatial multiplexing systems," *IEEE Communications Letters*, vol. 6, no. 11, pp. 491–493, Nov 2002.

[12] M. Porter, "Bellhopcode," *[online] Available: http://oalib.hlsresearch.com/Rays/index.html*.

[13] P. Qarabaqi and M. Stojanovic, "Statistical characterization and computationally efficient modeling of a class of underwater acoustic communication channels," *IEEE Journal of Oceanic Engineering*, vol. 38, pp. 701–717, 2013.

[14] M. Stojanovic, "On the relationship between capacity and distance in an underwater acoustic communication channel," in *Proc. of the ACM International Workshop on Underwater Networks (WUWNet), Los Angeles, CA, pp. 41–47, Sept. 2006*, Sept. 2006, pp. 41–47.

[15] P. Bouvet and A. Loussert, "Capacity analysis of underwater acoustic MIMO communications," in *IEEE OCEANS*, May 2010, pp. 1–8.